MARCH 1980 PPPL-1520
UC-20f

THE QED-1 DEVICE AND MEASUREMENTS OF GETTERING EFFICIENCY FOR A SIMULATED DIVERTOR PLASMA

BY

D. K. OWENS AND M. YAMADA

PLASMA PHYSICS LABORATORY

PRINCETON UNIVERSITY
PRINCETON, NEW JERSEY

This work was supported by the U. S. Department of Energy Contract No. ET-76-C-02-3073. Reproduction, translation, publication, use and disposal, in whole or in part, by or for the United States Government is permitted.

THE QED-1 DEVICE AND MEASUREMENTS OF GETTERING EFFICIENCY FOR A SIMULATED DIVERTOR PLASMA

D. K. Owens and M. Yamada

Plasma Physics Laboratory, Princeton University
Princeton, New Jersey 08544

ABSTRACT

The QED-1 device at PPL has provided gettering efficiency data for neutralized hydrogen plasma on titanium. The hollow-anode arcjet produces a plasma column 1 cm in diameter with $10^{12} < n_e < 10^{15}$ cm^{-3} and $T_i \lesssim T_e = 3\text{-}10$ eV, confined by an axial magnetic field of 1-6 kG. The gettering measurements are based on monitoring neutral gas density with respect to time in the divertor simulation chamber of QED-1. The present results indicate that the plasma particles lose their charge and most of their energy when they strike the neutralizer plate.

INTRODUCTION

With the recent achievement of containing higher-β plasmas in magnetic fusion devices, interest in the experimental investigation of MHD (macro) and kinetic (micro) stability of finite-β plasmas ($10^{-3} < \beta \leq 1$) has greatly increased. The construction of a long pulse-length or steady-state quiet, high density plasma device would greatly contribute to the better understanding of plasma stability relevant to magnetic fusion research.

The encouraging results of the recent magnetic divertor[1] tests in tokamaks has created an interest in divertor simulation in which the environment of a divertor plasma is reproduced as a slender tube terminated by a collector plate. In this kind of plasma one would be able to investigate particle and heat transport in a flowing plasma which simulates the divertor scrape-off regime and obtain data on particle gettering, plasma collection, sputtering yield, and plasma-neutral gas interaction. An energetic arc device was constructed at PPL in 1976 to provide relevant experimental data in these research areas.

The QED-1 (Quiet-Energetic-Dense) device produces a hot ($T_e \simeq$ 1-10 eV) isothermal, current-free plasma with an arcjet plasma gun. In this machine, a 1-2 cm-diameter plasma streams along the magnetic field into a burial chamber where the plasma recombines on the neutralizer plate and the resulting neutral gas is pumped away. High speed differential pumping ensures low background-pressure in the experimental region, and thus uniform plasma. Plasma density of $n_e = 10^{12}$-10^{15} cm^{-3} and temperature T_e = 3-10 eV have been obtained for various gas discharges, i.e. H_2, D_2, He, and Ar. The anode of the arcjet

gun is made of oxygen-free high conductivity copper with a 1.6 mm thick wall between the vacuum and water cooling channel. The cathode is 3% thoriated tungsten, 9.5 mm diameter, the same dimension as the anode orifice.

The gettering experiment on QED-1 was performed to determine the type and energy of neutral gas which comes off the neutralizer plate and measure the sticking coefficient on titanium of the resulting gas. Although G. Martin[2] has set a lower limit of 10% * for the sticking coefficient of room temperature atomic hydrogen on Ti films, the composition of a neutralized H plasma is not known.

For the measurements, the QED arcjet is used to produce a 3-10 eV atomic hydrogen plasma which is neutralized by striking a cold neutralizer plate. The resulting gas is then used as a known source in a classical pumping speed measurement. It appears that the gas which comes off the neutralizer plate is mostly cool molecular hydrogen.

Section II discusses the mechanical and operational aspects of the machine. Section III presents data on the various plasmas which have been produced in QED-1, and Section IV describes the titanium-film gettering experiment.

---

*Martin did not take into account that an ionization gauge is less sensitive to H that H_2. The reduced sensitivity results in a 10% lower limit for the sticking coefficient, rather than 30%.

II. Description of the QED-1 Device.

The four-stage differentially pumped arcjet system, which was constructed at UCLA[3] similar to the TPD device developed at IPP,[4,5] Nagoya, Japan, generated remarkably high density plasma in steadystate. The present QED-1 device is an improved version of the UCLA device with higher pumping speed, anode-cooling capacity and diversified operation modes.

The normal configuration of the QED-1 device is shown in Fig. 1. It can be modified in several ways, such as placement and number of limiters, magnetic field, and layout of the experimental area at the neutralizer-plate end of the machine. Such modifications permit optimum design for different experiments. In this Section each of the major components are described.

II-A. Construction of Machine.

The linear magnetic field is produced by two sets of pancake coils, L-2 standard coils (with 25 cm bore), and larger, Q-1 test coils (with 60 cm bore). The field can be varied from 1 kG to 6 kG with an on-axis ripple of ± 2.5%.

The water-cooled vacuum chamber is stainless steel with gold-seal flanges. As shown in Fig. 1, there are four access areas. Position #1 is a four-port cross with 2" diameter flanges. Positions #2-4 have two, 2" diameter flanges on the upper and lower surfaces of the vacuum vessel. In addition to the 2" flanges positions #3 and #4 have 6" diameter flanges in the horizontal plane with a field of view across the diffusion pumps through the plasma. These ports are useful for spectroscopy and large probe drives.

In order to obtain low neutral pressures in the experimental area during arc operation, high-speed differential pumping is employed. The vacuum chamber is divided into four regions by cooled, electrically isolated limiters which make a tight seal at the wall and have a 2 cm diameter hole in the center. Plasma, flowing along the magnetic field, passes directly through these holes. Neutral gas also flows through the holes, but is not confined by the magnetic field so that the flow is effusive and not directed. By pumping on each chamber (differential pumping) with pumps of sufficient speed ($\sim 10^3$ ℓ/sec), it is possible to obtain a pressure drop of 1-2 orders of magnitude across each limiter and 10^{-4}-10^{-6} torr pressures in the experimental area.

To maintain high pumping speed over the pressure range of 10^{-6} torr to several torr in QED-1, two types of pumps are necessary: standard diffusion pumps for pressures less than 10^{-3} torr and booster pumps (called ring-jet pumps) for pressures greater than 10^{-3} torr. A booster pump and a diffusion pump are similar in construction, the difference being that diffusion pumps are optimized for operation in the molecular flow regime while booster pumps are optimized for the viscous flow regime.

The water-cooled, copper neutralizer plate is electrically isolated from the machine and can be biased to collect ion or electron current.

The shutter is a water-cooled copper plate which is used to stop plasma flow without shutting off the arcjet itself. It can be moved into the plasma in less than 200 ms and removed from the plasma in less than 50 ms. This feature was necessary

for the gettering experiment and is useful for density measurements with the 2 mm microwave interferometer.

The arcjet gun is shown in Fig. 2. The anode is made of oxygen-free high conductivity copper with a 1.6 mm thick wall between the vacuum and water cooling channel. The vacuum seal between the cooling channel and vacuum is made with two "O-rings" shown as black ovals in Fig. 2. The cathode is 3% thoriated tungsten, 9.5 mm (3/8") diameter, the same dimension as the anode orifice.

Gas flows into the arc region through a .38 mm wide, 6.35 cm diameter annular orifice. Any gas can be used to form an arc except those gases which chemically attack the electrode surfaces at high temperatures. So far, plasmas have been generated using hydrogen, deuterium, helium, and argon. For start-up, argon is always used since it readily forms an arc without damaging the anode. Other gases can then be slowly substituted for the argon.

II-B. Operation of Machine

The arcjet is powered by three, floating supplies in parallel: a high-voltage, low current starting supply; a medium current sustaining supply, and a high current supply. The starting supply is used for breakdown, and the sustaining supply maintains the discharge until the current from the main supply (connected through a blocking diode) is increased and the arc is operating in a stable high current, low voltage mode. A 1 farad, 380 V capacitor bank is also available for pulse experiments. Table I is a summary of typical arcjet operating conditions.

In discussing the physical limitations of the arcjet, it is important to have an idea of conditions in the arc region during normal operation. For the low pressure arc in the arcjet, most of the total arc current is carried by thermionic electrons emitted from the cathode [6] which requires the cathode surface to be molten in order to provide the 100A and greater currents needed. A simple calculation for a cooled cathode indicates that the ion bombardment which heats the cathode to the necessary temperature must supply about 800 W. The cathode is cooled to prevent the cathode support structure from becoming too hot and not to keep the cathode itself from overheating, since thermal radiation is sufficient to regulate cathode temperature. When the cathode-anode separation is large enough for proper electrode sheaths to form, only a small amount of tungsten is lost from the cathode although it is clear that the surface is molten since the end of the cathode develops a small protrusion after a short running time.

For a self-sustained, hot cathode arc, the cathode fall determines conditions in the arc. [6] The power to the cathode is only 800 W for stable operation, and the plasma striking the collector plate carries only a few hundred watts, hence all but about 1 kW of arc power is deposited on the anode or heats the gas in the anode chamber.

To prevent catastrophic anode failure, it is necessary to efficiently cool the anode. It is possible to calculate the cooling using published correlations [7] for water cooling provided the power deposition as a function of position on the anode is

known. Although we do not know the depositon profile, the cooling can be calculated for the worst case situation in which essentially all the power to the anode is deposited in the narrow throat region of the anode. This situation is expected to occur under low pressure, high magnetic field conditions, i.e., just the conditions which produce the hottest plasmas. The cooling calculation for this case indicates that the maximum power which can be removed from the anode is 10 kW. At these power levels (2.6 kW/cm^2), nucleate boiling at the water-copper interface is extremely important in increasing flow turbulence and enhancing thermal transport.[8] Temperature induced mechanical stresses in the anode could also be a problem at these power levels[9] leading to anode failure. For higher gas pressures and lower fields, where the power is expected to be deposited over a larger area of the anode, higher power levels up to 20 kW can be achieved without failure.

III. Plasma Properties of the QED-1 Device.

For the working gases H_2, D_2, He, and Ar, the plasma properties of the present steady-state plasma have been extensively measured. The determination of plasma parameters has often been made using more than two diagnostic techniques. A list of diagnostics used for each plasma parameter is shown in Table 2. Despite earlier estimates, Langmuir probes (cooled and non-cooled) can withstand high density Argon plasma of $n_e \geq 10^{14} cm^{-3}$. For density measurements of He^+, H^+, and D^+ plasmas ($n_e \geq 10^{14} cm^{-3}$),

we have used a swept probe which can radially traverse the plasma column within a few seconds.

Fig. 3(a) and Fig. 3(b) show typical radial density distributions and potential profiles for high-current Argon discharges. In order to obtain high density Argon discharges, the discharge current and the confining magnetic field were kept high ($B_o \geq 5$ kG), the highest density obtained being $2 \times 10^{15} cm^{-3}$. The absolute value of the density was determined with a far-infrared laser (CH_3OH, $\lambda = 119\ \mu$) interferrometer which was developed for the PDX diagnostics.[10] As shown in Fig. 4, the electron density increases almost proportionally to the gas-flow feed rate (Q) to the plasma gun, up to Q ≈ 3 torr ℓ/sec but decreases as Q increases further. Fig. 5 and Fig. 6 present the plasma density for hydrogen and deuterium discharges, respectively, for various gas-feed rates as a function of discharge current. Fig. 7 depicts the dependence of plasma density on magnetic field. As is shown in these figures, a high-current discharge in a large magnetic field produces a high density plasma for the working gases H_2, D_2. Long-term (>5 hrs) operation of high-current, high-field discharges can damage the anode resulting in catastrophic destruction of the gun. Under normal conditions ($I < 200A$, $B \leq 3$ kG), the anode can last as long as 200 hours.

The electron temperature of the present plasma is not much different from that of a standard arc discharge. The electrons ejected from the hollow anode have a temperature of $2\ eV < T_e \leq 10\ eV$ and extract ions by an ambipolar diffusion potential. The plasma flow velocity measured in the linear region between the

gun and the final chamber was of the order of 1/2 ~ 1/4 C_s, where C_s is the ion sound velocity. The ions, which are as cold as room temperature in the arcjet nozzle ($p > 1$ Torr), are heated by collisions with electrons during their drift to the experimental chamber. In high-density operation, the ion temperature has been determined to be roughly equal to the electron temperature as measured by doppler broadening spectroscopy. Fig. 8 presents the measured electron temperature for Argon discharges as a function of gas flow. One sees a good agreement between the probe measurements and the spectroscopic measurements of S. Suckewer.[11] For the spectroscopic measurements, the line intensity from Ar II 4806Å, 4865Å, 3957Å, 3480Å, 3480.6Å and the impurity lines C II 4267Å, C III 2297Å have been monitored. A low gas flow, high-current, high-field discharge tends to generate a high temperature plasma. Fig. 9 shows the dependence of T_e for H_2 discharges and the optimum gas flow rate is found to be 10 Torr ℓ/sec with $T_e \simeq 10$ eV. Fig. 10 gives the dependence of T_e on the confining magnetic field, B, for hydrogen discharges of 200 Amp and a gas-feed rate of 11 torr ℓ/sec.

Helium discharges have also been successfully produced with plasma properties similar to those of H_2 discharges, except that helium discharges tend to have higher electron temperatures. The plasma density range of $10^{12}cm^{-3} < n_e < 5 \times 10^{14}cm^{-3}$ has been obtained for this gas.

The base pressure in the vacuum vessel was below 2×10^{-6}torr before the gettering experiment. The pressure in the experimental

chamber during plasma discharge was of the order of 10^{-4}torr. Concentration of impurity atoms and molecules in the plasma was monitored using a spectroscopic method and found to be very small; normally it was less than 0.1%. The degree of ionization in the hydrogen plasma has also been checked by means of probes and spectroscopy and the plasma was found to be more than 50% ionized.

IV. Gettering Experiment.

As originally planned, the gettering experiment on QED-1 was supposed to measure the sticking coefficient of 3-10 eV neutral atomic hydrogen on titanium films for the purpose of simulating getter pumping in the divertor region of PDX. The assumption that a 3-10 eV atomic hydrogen plasma will produce an equally hot neutral gas upon striking a metal plate has proven to be incorrect, as the high pumping speeds predicted for 3-10 eV atomic hydrogen have not been observed. Instead, the pumping speed on Ti of the neutral gas evolving from the neutralizer plate combined with published values of the sticking coefficient of room temperature molecular and atomic hydrogen on Ti have been used to roughly establish the composition and energy of the neutral gas.

For the experiment, the QED arcjet is used to produce a 3-10 eV atomic hydrogen plasma which is neutralized by striking a cold metal plate located in a large chamber (Fig. 11). The resulting gas is then used as a known source in a classical pumping speed measurement.

IV-A. Theory

The theory which is used to interpret the sticking coefficient results should be a kinetic theory which takes into account that fast particles are pumped more rapidly than slow particles. This is important since certain kinds of measurements are sensitive to the velocity distribution function of the particles in the chamber. However, since the gas in the chamber is concluded to be cool, the usual pumping equation adequately describes the situation. Then

$$V\frac{dn}{dt} = -Fn - \frac{\alpha v_A A}{4} n + \left(1 - \frac{\alpha A}{A_o}\right) N \quad , \tag{1}$$

where

V = chamber volume

n = particle density

F = diffusion pump speed

α = sticking coefficient

$v_A = (8\ kT/M\pi)^{1/2}$

A = area of Ti film

A_o = chamber area

N = particle influx rate

The factor $(1-\alpha A/A_o)$ takes into account those particles which stick to the Ti on the first bounce and do not contribute to the particle density as measured by a gauge shielded from the neutralizer plate. In general, α depends on the amount of hydrogen which has been absorbed by the titanium.

For the gettering experiment, the source function, N, is a step (50 ms rise time) obtained by opening the shutter. N is obtained by measuring the ion saturation current to the end plate. If the H^+ plasma recombines on the end plate producing H_2, then half the ion saturation current is used to determine N. With this source the pumping speed can be measured three ways:

1) Pumping time constant

$$\frac{1}{\tau} = \left(F + \frac{\alpha v_A A}{4}\right)/V \quad . \tag{2}$$

2) For times long compared to the above time constant, the steady-state solution can be used

$$n = \frac{\left(1 - \alpha A/A_o\right)N}{F_{PUMP} + \frac{\alpha v_A A}{4}} \quad . \tag{3}$$

3) Using (3) with and without gettering and constant N, one obtains

$$\frac{n_o}{n_G} = \frac{1}{\left(1 - \alpha A/A_o\right)} \left(1 + \frac{F_{Ti}}{F_{PUMP}}\right) \quad , \tag{4}$$

where n_o = density without gettering

n_G = density with gettering

$F_{Ti} = \alpha v_A A/4$.

For the QED-1 parameters, Table 3, the time constant measurement is difficult so that the second and third methods were used.

IV-B. Instrumentation.

The instrumentation consisted of a glass enclosed ionization gauge connected to the gettering chamber by glass tabulation and a power supply and ammeter for measuring the ion saturation current to the neutralizer plate. We attempted to use a nude ionization gauge to measure the gas density directly but found the nude gauge to be sensitive to residual plasma in the chamber and hence unreliable.

The enclosed gauge was calibrated for H_2 using a Baritron capacitance manometer. The calibration for H was inferred from the H_2 and H ionization cross-sections at 100 eV. The gauge is 2.6 times less sensitive to H than H_2. The change in sensitivity with magnetic field was calibrated and taken into account.

In steady-state or for density changes slow compared to the enclosed gauge time constant, the requirement of influx to the gauge equal to outflux from the gauge yields

$$n_g = n\left(\frac{v_A}{v_o}\right) \quad , \tag{5}$$

where

n_g = density in gauge

n = density in gettering chamber

$v_A = (8\ kT/M\pi)^{1/2}$, T = chamber gas temperature

$v_o = (8\ kT_o/M\pi)^{1/2}$, T_o = gauge gas temperature .

It is usually assumed that the hot gas which enters the gauge cools to room temperature by the time it reaches the gauge. If n were obtained independently, e.g. n = N/F in steady-state, v_A/v_o could be inferred from the enclosed gauge response.

Combining Eq. 3 with Eq. 5 and assuming $F_{Ti} >> F_{PUMP}$ one obtains

$$\alpha = N/(An_g\ v_o/4) \quad , \tag{6}$$

or from Eq. 4 and QED-1 parameters

$$\frac{F_{Ti}}{F_{PUMP}} = \frac{n_o}{n_G} - 1 \quad . \tag{7}$$

IV-C. Results.

To perform the measurements, the arcjet was turned on and allowed to run until a stable discharge was well established. The plasma was allowed to enter the gettering chamber during this time to ensure that the Ti film left from previous runs was completely saturated and hence had no pumping capability. The value of n_o, gauge density with plasma but no gettering, was recorded along with the ion saturation current to the neutralizer plate. The electron temperature of the H^+ plasma was measured and found to be 3 eV in front of the neutralizer plate.

The shutter was then closed and Ti deposited on the gettering chamber walls. After a sufficient amount of Ti had been deposited the shutter was opened (typically for less than 2-3 seconds) and the pressure in the gauge recorded during the pressure rise and until steady state had been reached. The shutter was then closed. More Ti was deposited and the measurements repeated. The density rise in the gettering chamber is shown with and without titanium deposition in Fig. (12). In the upper trace the density increases with a time constant of approximately .15 s, determined by the volume of the chamber and pumping speed of the diffusion pumps. In the lower trace, titanium has been deposited and the pumping speed is on the order of 50 times greater than with diffusion pumps alone. The initial rate of rise is limited by the opening time of the shutter (50 ms). The linear rise in pressure after .1 s is due to a decrease in the pumping speed of the titanium film.

In Figure (13) α, as determined by Eq. 6 is plotted vs F_{Ti}/F_{PUMP} (Eq. 7) from our data. To calculate α from Eq. 6, it was assumed that the gas in the gauge was at room temperature, hence these curves represent upper limits on α. A case not shown in Figure 13 is atomic hydrogen in the gettering chamber which recombines in the ionization gauge so that the gauge measures H_2. Assuming this model, α for atomic hydrogen would lie on the line for H_2 in Fig. 13. The first conclusion to be drawn is that the gas in the chamber is not atomic hydrogen as the sticking coefficient for H is always less than G. Martin's lower limit of 10%.

Assuming the gas in the chamber to be H_2, one can calculate v_A/v_o, the ratio of the thermal speed of the gas in the chamber to the speed of the gas in the gauge. The pumping speed of the diffusion pumps was measured without gettering by opening the shutter and measuring the time constant of the pressure rise. Given the pumping speed, either F_{Ti} or F_{PUMP}, and the particle influx rate, N, from the ion saturation current to the end plate, v_A/v_o follows from Eq. 5. With gettering we find

$$v_A/v_o = 2.17 \pm .43 \text{ and}$$

without gettering

$$v_A/v_o = 2.45 \pm .1 \ .$$

Limits can be set on v_o: the lower limit corresponding to room temperature and the upper limit if we assume that the maximum α we observe corresponds to a sticking coefficient of 3%[12,13] which makes v_o about 2.3 times room temperature. The gas which comes off the neutralizer plate then has a mean energy, E:

$$.1 \text{ eV} \leq E \leq .8 \text{ eV} .$$

The energy of the ions striking the neutralizer plate is estimated to be at least 10 eV.

A final result is shown in Fig. (14), where the sticking coefficient (assuming room temperature H_2) is plotted versus monolayers of freshly deposited titanium. As can be seen, full pumping speed is not attained until ~2000 monolayers of Ti are deposited.

The estimates of gas energy and composition which we have made are of course indirect and open to criticism. However, as a simulation of divertor pumping, we have the result that a 2000 monolayer thick titanium film pumps a neutralized hydrogen plasma at 7.8 ℓs^{-1} cm^{-2}.

IV-D. Conclusion.

The QED-1 hollow-anode arcjet device has produced a high density plasma column of $n_e = 10^{12} - 10^{15}$ cm^{-3} and $T_i \leq T_e = 3\text{-}10$ eV. In this device, we have measured the pumping speed of titanium films for a neutralized hydrogen plasma as 7.8 $\ell s^{-1} cm^{-2}$. We estimate that when a H plasma (3-10 eV) is neutralized on a metal plate, cool (.1-.8 eV) molecular hydrogen is formed.

Furthermore, we have concluded that two thousand monolayers of titanium are necessary to obtain an optimum sticking coefficient for hydrogen.

ACKNOWLEDGMENTS

This work was supported by the U.S. Department of Energy Contract No. DE-AC02-76-CHO 3073.

It is our great pleasure to thank Mr. L. Gereg for his significant contribution to the fabrication of the present device. We also would like to thank Dr. H. Hendel, Dr. D. Jassby, Dr. N. Luhmann, and Dr. T. H. Stix for quite useful advice. Thanks are also due to Mr. Wen Hsu who has accurately calibrated the plasma density of the QED-1 device.

REFERENCES

[1]J. W. M. Paul et al., in Proc of 6th Int. Conf. on Plasma Physics and Controlled Nucl. Fusion., IAEA-CN-35/A17 Berchteogaden (1976) H. Maeda et al., abid IAEA-CN-35/A17 (1976).

[2]G. D. Martin, in Symposium on Engineering Problems of Fusion Research, 6th, San Diego CA., 1975, New York, IEEE Nuclear and Plasma Sciences Society (1976).

[3]J. T. Tang et al., J. Appl. Phys. 46, 3376 (1975).

[4]M. Otsuka et al., Proceedings of the 7th Int. Conf. on Phenomena in Ionized Gases 1, 420 (1966).

[5]M. Otsuka et al., IPP Annual Report, IPPJ-1891974, p. 59 (April 1973-March 1974).

[6]S. C. Brown, Basic Data of Plasma Physics, 1959. Cambridge, MIT Press (1959).

[7]R. H. Novis et al., eds., Heat Transfer and Fluid Flow Handbook. General Electric Co., Corporate Research and Development, Schenectady, N.Y. (1970).

[8]W. H. McAdams, Heat Transmission. 3rd ed., New York, McGraw-Hill (1954).

[9]S. P. Timoshenko and J. N. Goodier, Theory of Elasticity, 3rd ed., New York, McGraw-Hill (1970).

[10]D. Mansfield et al., Bull. Am. Phys. Soc, 24, 932 (1979).

[11]S. Suckewer, NUKEEONIKA-TOM 14, 893 (1969).

[12]P. J. Harra, J. Vac. Sci. Tech., Vol. 13, No. 1 (Jan, Feb, 1976) 471.

[13]R. E. Clausing in 1961 Transactions of the Eighth National Vacuum Symposium and the Second International Congress on Vacuum Science and Technology, L. P. Preuss, Editor Pergamon Press, New York (1962).

TABLE 1

Anode Cooling	10 gpm, 300 psi deionized water
Cathode Cooling	300 psi deionized water ~ 10 gpm
Maximum Power for Extended Lifetime (> 10 hrs.)	$P \leq 10$ kW (low density) $P \leq 20$ kW (high density) $I \leq 200$ A, $V \leq 60$ V
Lifetime for Power Levels Above 20 kW	$\leq$ 2-3 hrs.
Main Power Supply	0-1000 A, 120 V
Ballast Resistor	.4 Ω
Magnetic Field	1-6 kG, ± 2.5% Ripple

Table 2. Diagnostics for QED-1 Plasma

Plasma Parameters	Regime	Diagnostics
Density ($n_e = n_i$)	$10^{11}cm^{-3} < n_e \leq 5\times10^{14}cm^{-3}$	Probes
	$10^{13}cm^{-3} < n_e \leq 10^{14}cm^{-3}$	2 mm Microwave Interferometer
	$10^{14}cm^{-3} < n_e$	Infrared laser Interferometer
	$10^{13}cm^{-3} < n_e < 10^{15}cm^{-3}$	Spectroscopy
Electron Temperature T_e	.5 eV $< T_e <$ 10 eV	Spectroscopy Probes. Whistler-wave dispersion
Ion Temperature T_i	.5 eV $< T_i <$ 10 eV	Doppler broadening
Plasma Flow	$u = \frac{1}{2} - \frac{1}{4}\sqrt{\frac{kT_e}{M_i}}$	Collector Current
Impurity level	$\frac{n_i}{n_e} < 0.01$	Spectroscopy

TABLE 3

GAS	H	H_2
kT	1/40 eV	1/40 eV
v_A	2.5×10^5 cm/s	1.77×10^5 cm/s
α	$\geq$ .1	.03
A	2×10^4 cm^2	2×10^4 cm^2
V	2.2×10^5 cm^3	2.2×10^5 cm^3
SPEEDS		
F_{PUMP}	1.5×10^6 cm^3/s	1.5×10^6 cm^3/s
$\tau_1 = V/F_{PUMP}$	.15 s	.15 s
$\alpha v_A A/4$	$\geq 1.25 \times 10^8$ cm^3/s	2.66×10^7 cm^3/s
$\tau_2 = V/F_{Ti}$	$\leq$ 1.8 ms	8.3 ms

FIGURE CAPTIONS

Fig. 1. Normal QED-1 Machine Configuration.

Fig. 2. QED-1 Arcjet. The dark ovals are "O-ring " seals.

Fig. 3 a,b. Radial profiles of electron density and floating potential measured by probes for Argon plasma discharges. B = 5 kG, I = 400 A, Anode voltage = 50 V, Q denotes flow-rate of feed gas.

Fig. 4. Electron density obtained in the experimental chamber vs flow-rate of feed gas (Ar), B = 5 kG, I = 400A, 40 V < V_{Anode} < 60 V.

Fig. 5. Electron density of hydrogen plasma vs discharge current for various gas-feed rates; o 28 Torr·ℓ/sec, • 15 Torr·ℓ/sec, Δ 8 Torr·ℓ/sec. B = 2 kG. The absolute value was calibrated by 2 mm microwave interferrometer.

Fig. 6. Electron density of deuterium plasma vs discharge current for various gas-feed rates; • 20 Torr·ℓ/sec, o 12 Torr·ℓ/sec, Δ 6 Torr·ℓ/sec.

Fig. 7. Electron density of hydrogen plasma vs confining magnetic field.

Fig. 8. Electron temperature of Argon plasma vs flow-rate of feeding gas, B = 5 kG, I_p = 400 A. • denotes probe measurement, o denotes spectroscopic line intensity measurement by S. Suckewer.

Fig. 9. Electron temperature of hydrogen plasma vs flow-rate of feed gas. B = 3 kG, I_p = 200 A.

Fig. 10. Electron temperature of hydrogen plasma vs confining magnetic field. I_p = 200 A, V_{anode} = 55 V, flow rate of gas q = 11 torr·ℓ/sec.

Fig. 11. QED-1 Gettering Configuration.

Fig. 12a. Density rise in gettering chamber after shutter opens without Titanium gettering.

Fig. 12b. Density rise after shutter opens with gettering.

Fig. 13. Calculated sticking coefficient vs measured pumping speed for titanium gettering assuming room temperature gas.

Fig. 14. Sticking coefficient for H_2 on on titanium vs thickness of Ti film.

QED-I MACHINE CONFIGURATION

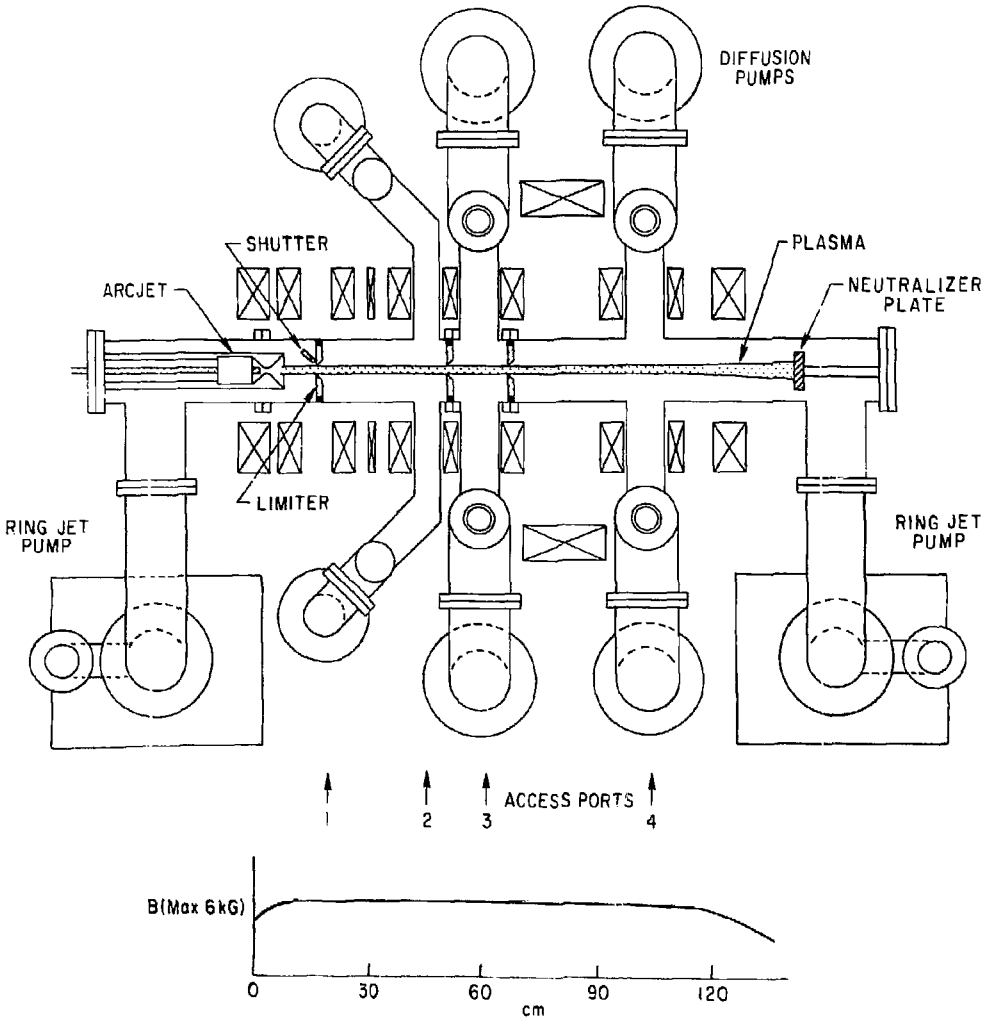

Fig. 1. (PPPL-783002)

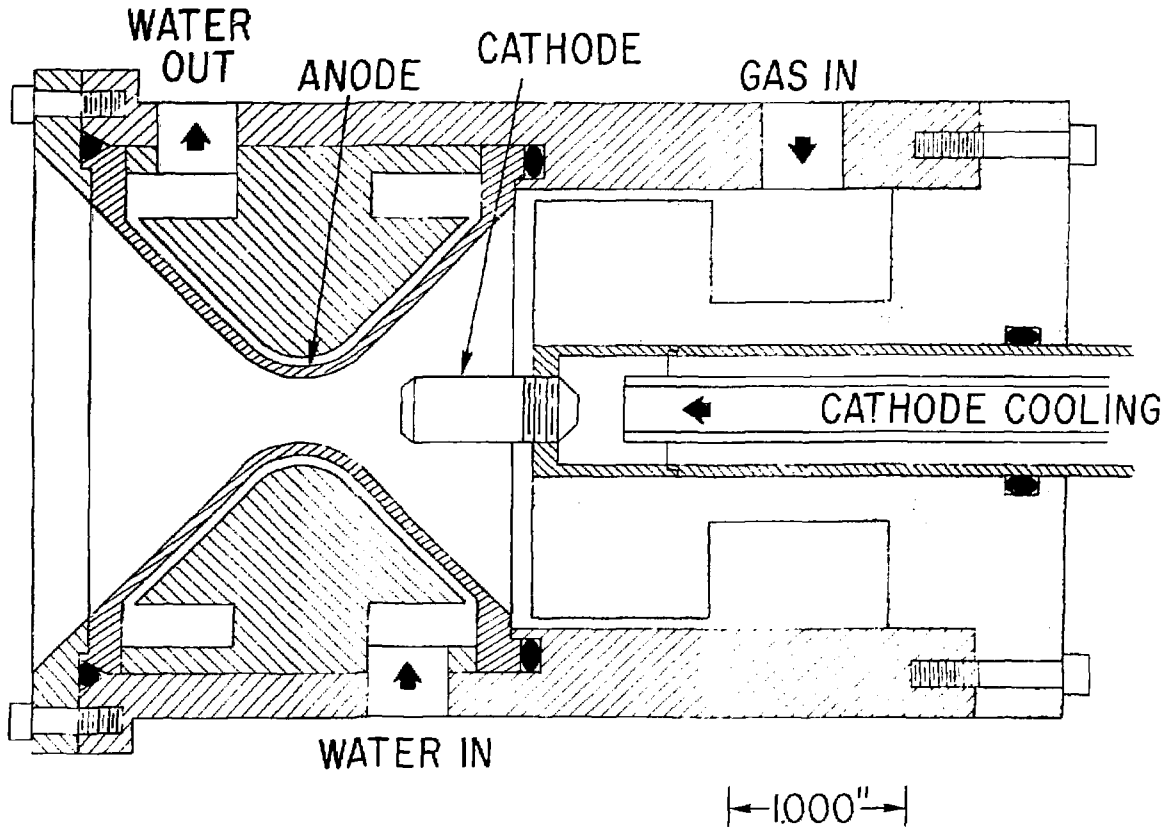

Fig. 2. (PPPL-783001)

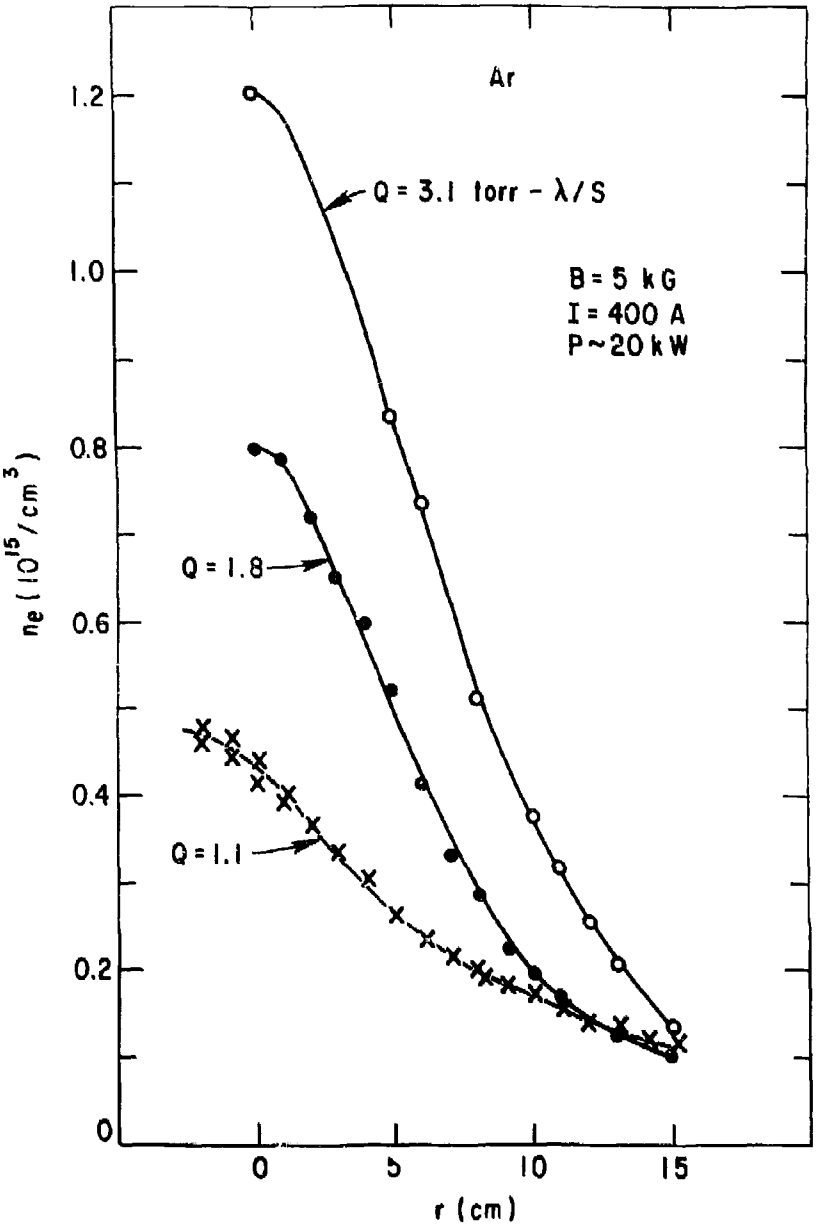

Fig. 3a. (PPPL-776036)

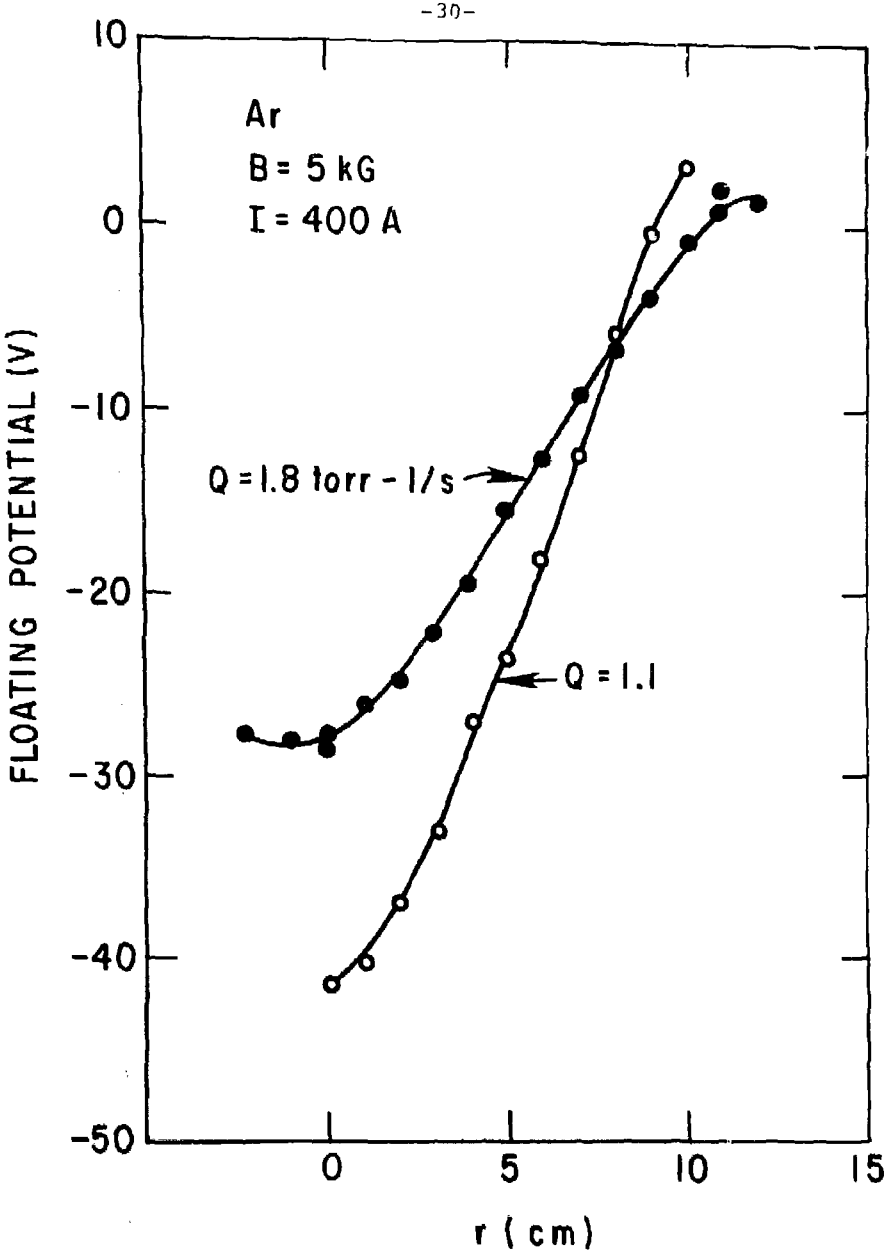

Fig. 3b. (PPPL-776037)

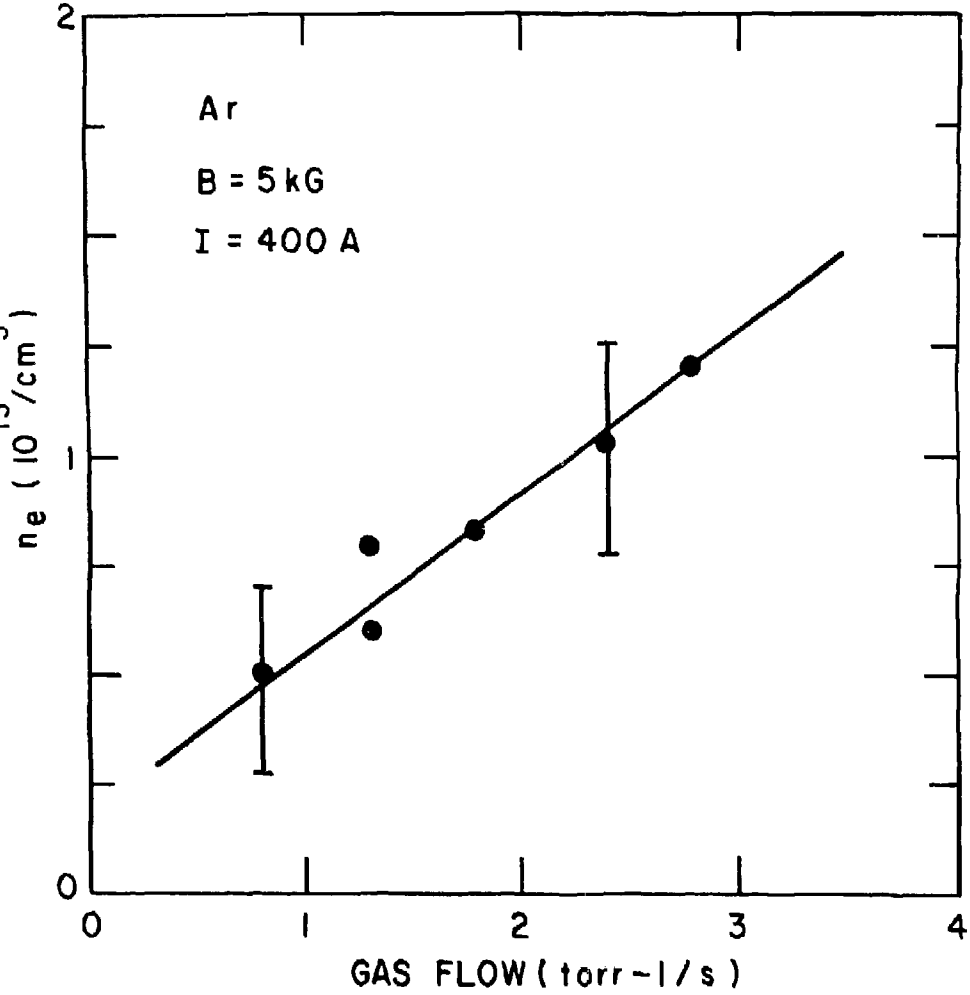

Fig. 4. (PPPL-804095)

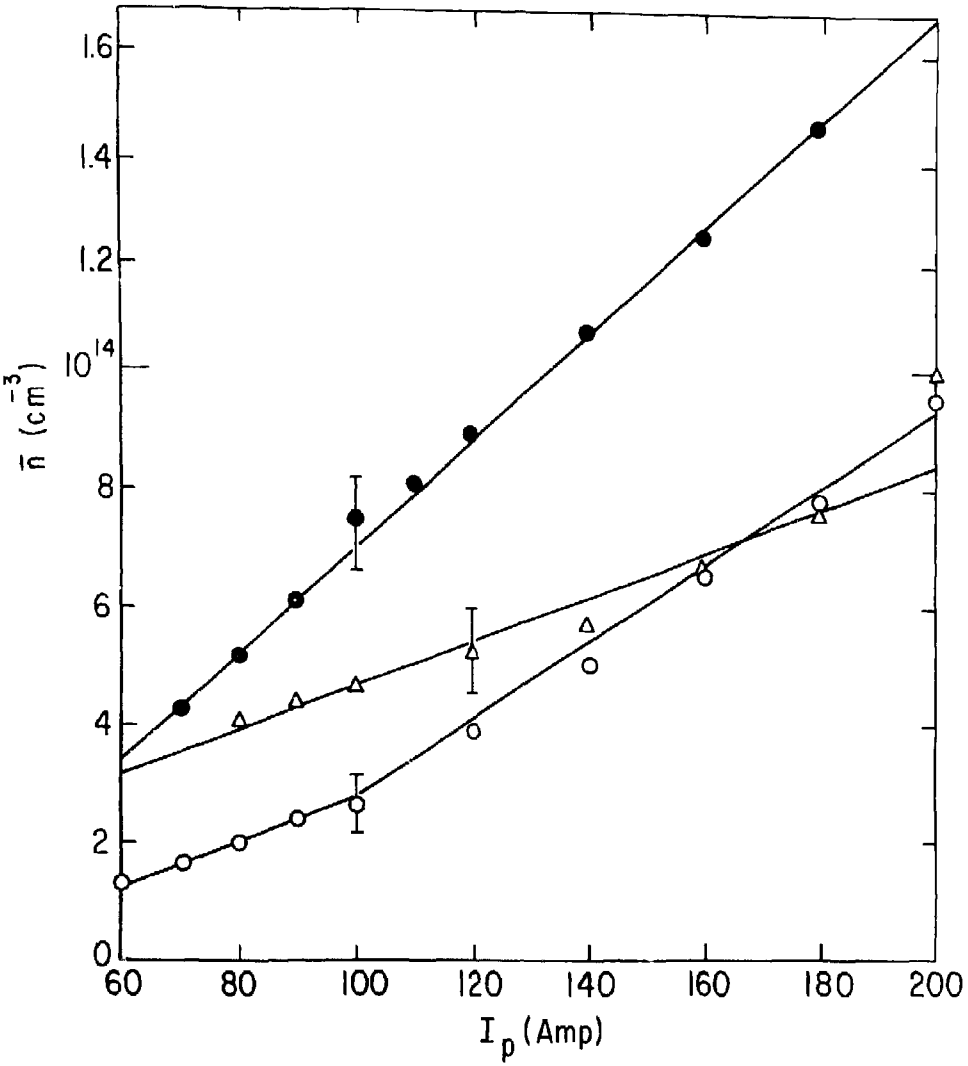

Fig. 5. (PPPL-803062)

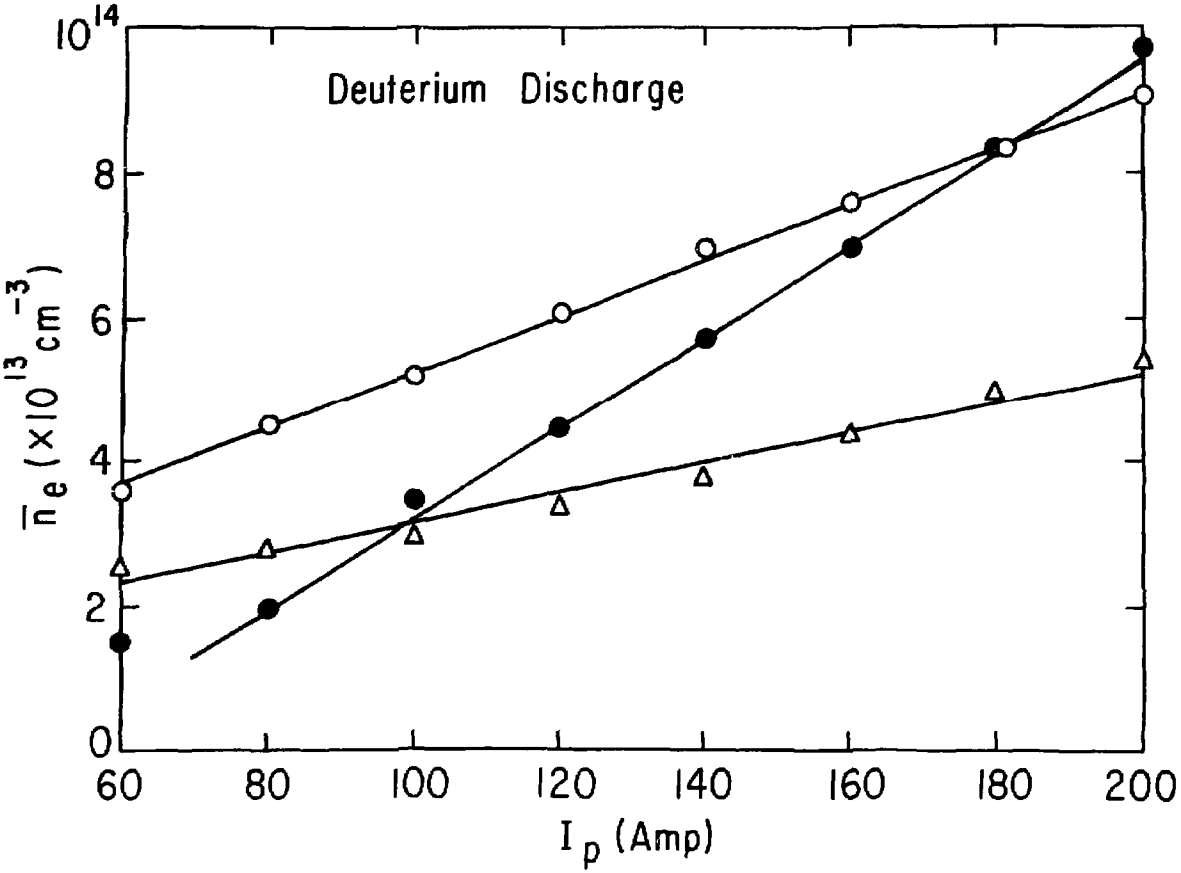

Fig. 6. (PPPL-803059)

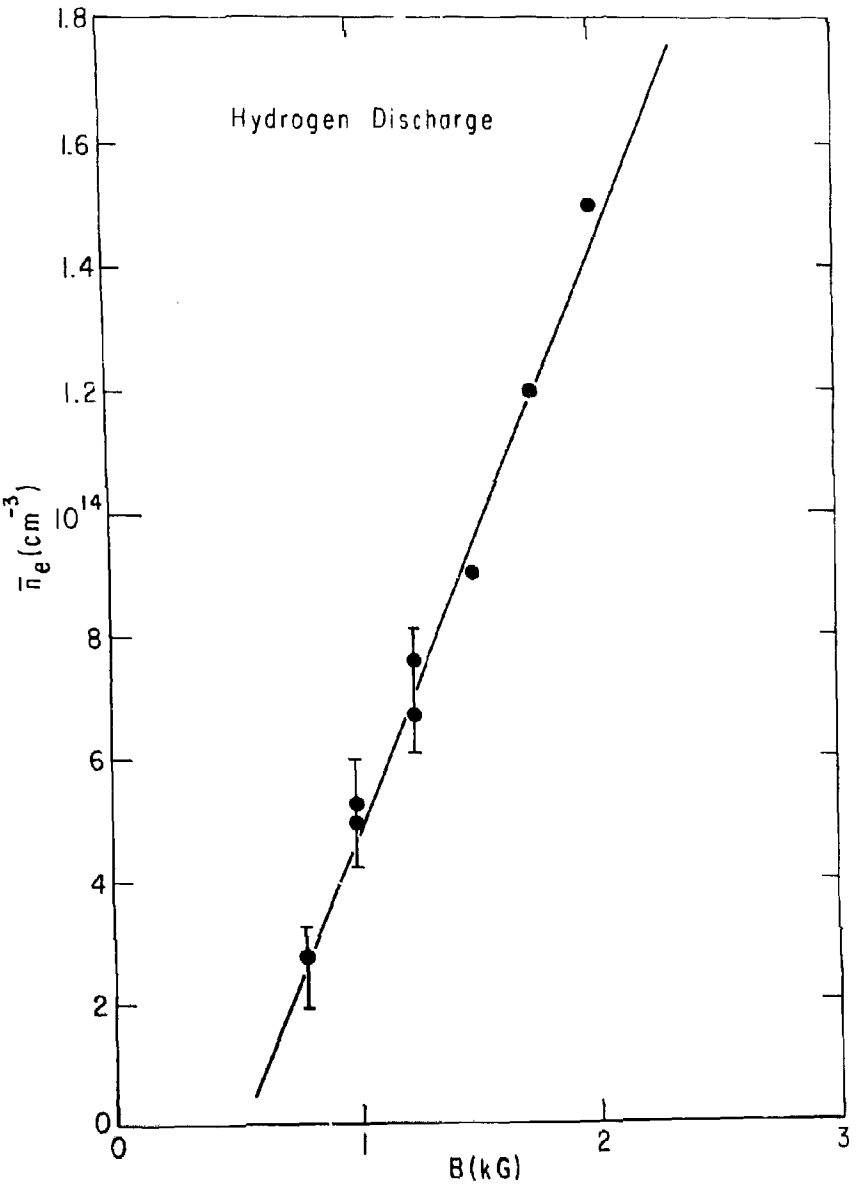

Fig. 7. (PPPL-803058)

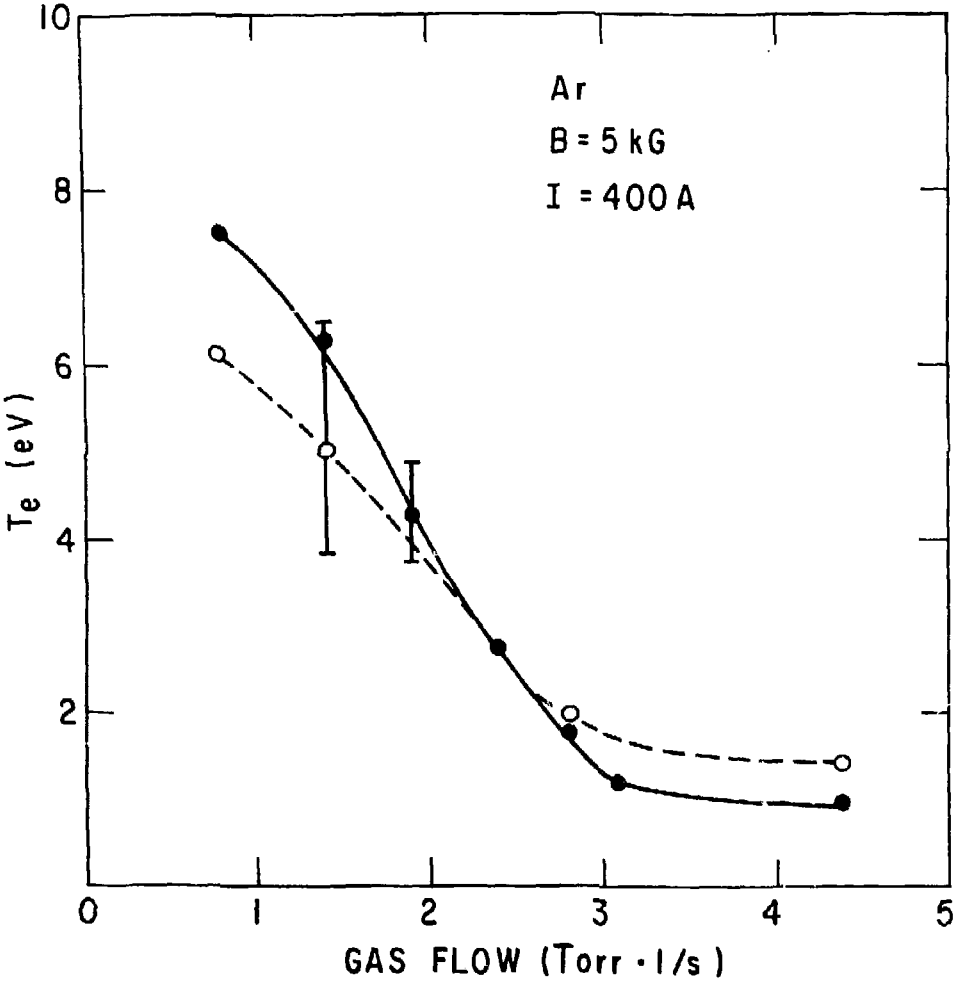

Fig. 8. (PPPL-803061)

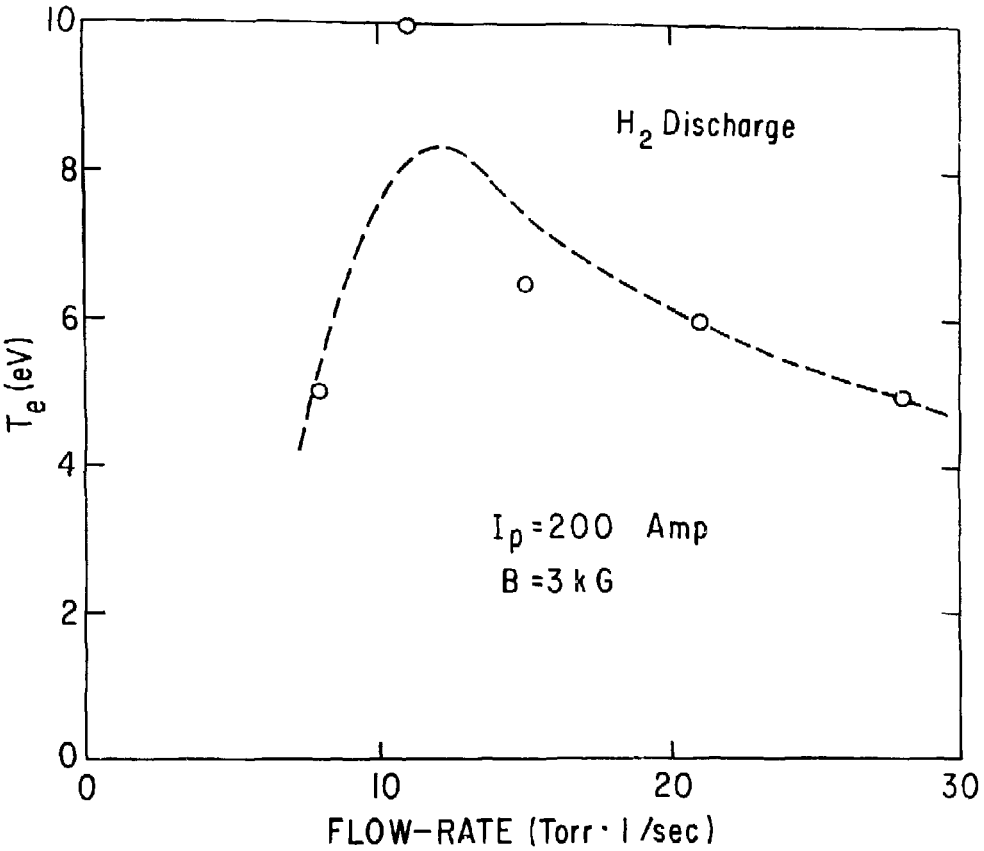

Fig. 9. (PPPL-803063)

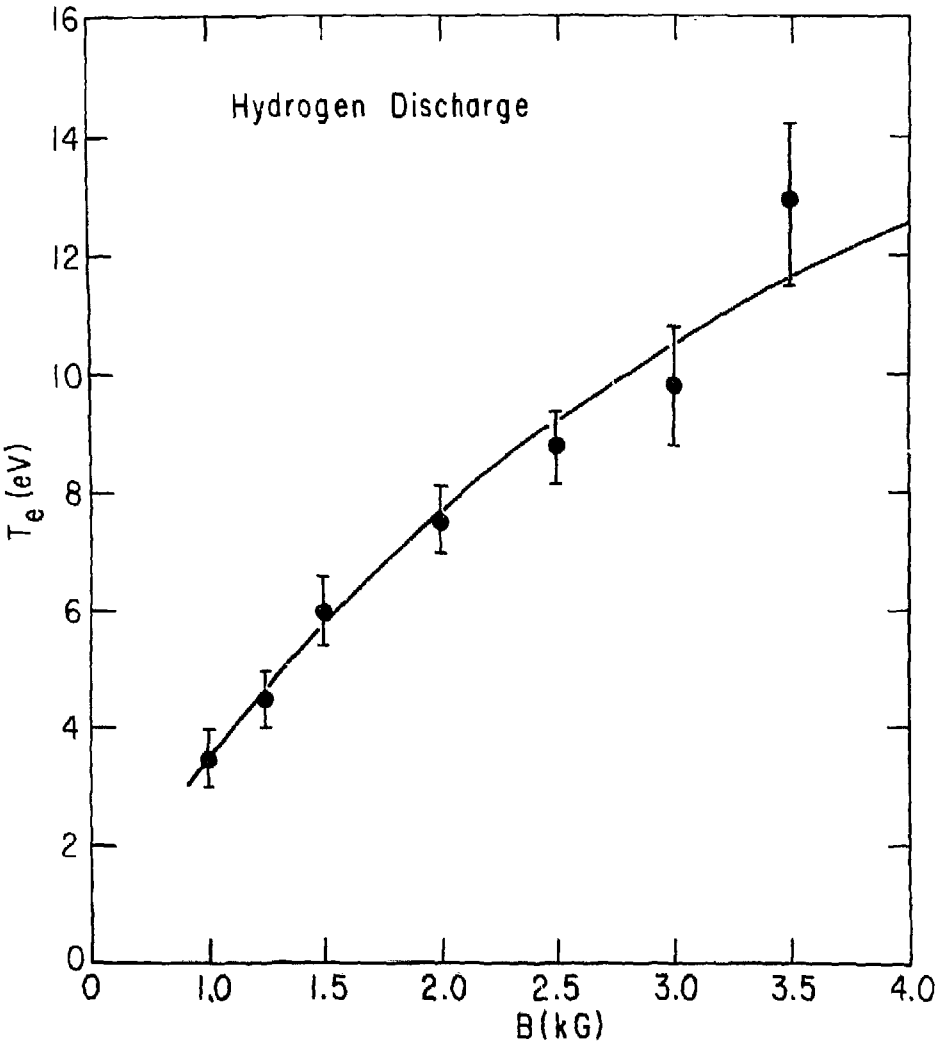

Fig. 10. (PPPL-803060)

QED-I GETTERING CONFIGURATION

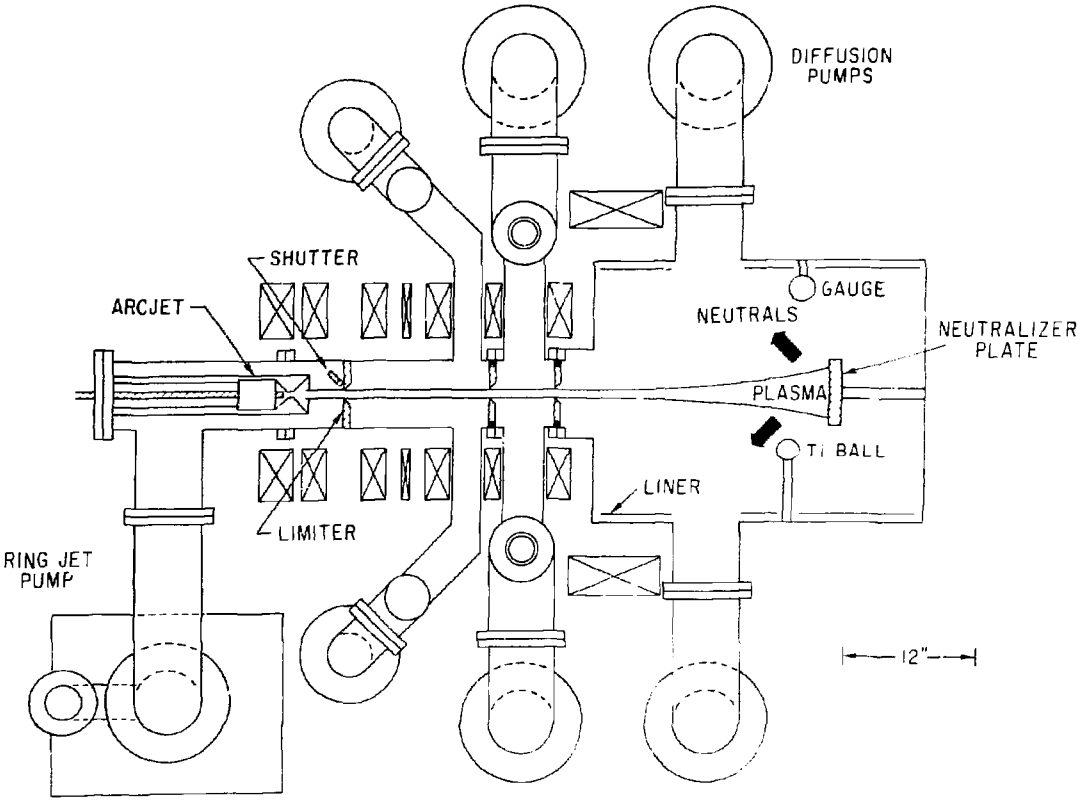

Fig. 11. (PPPL-776212)

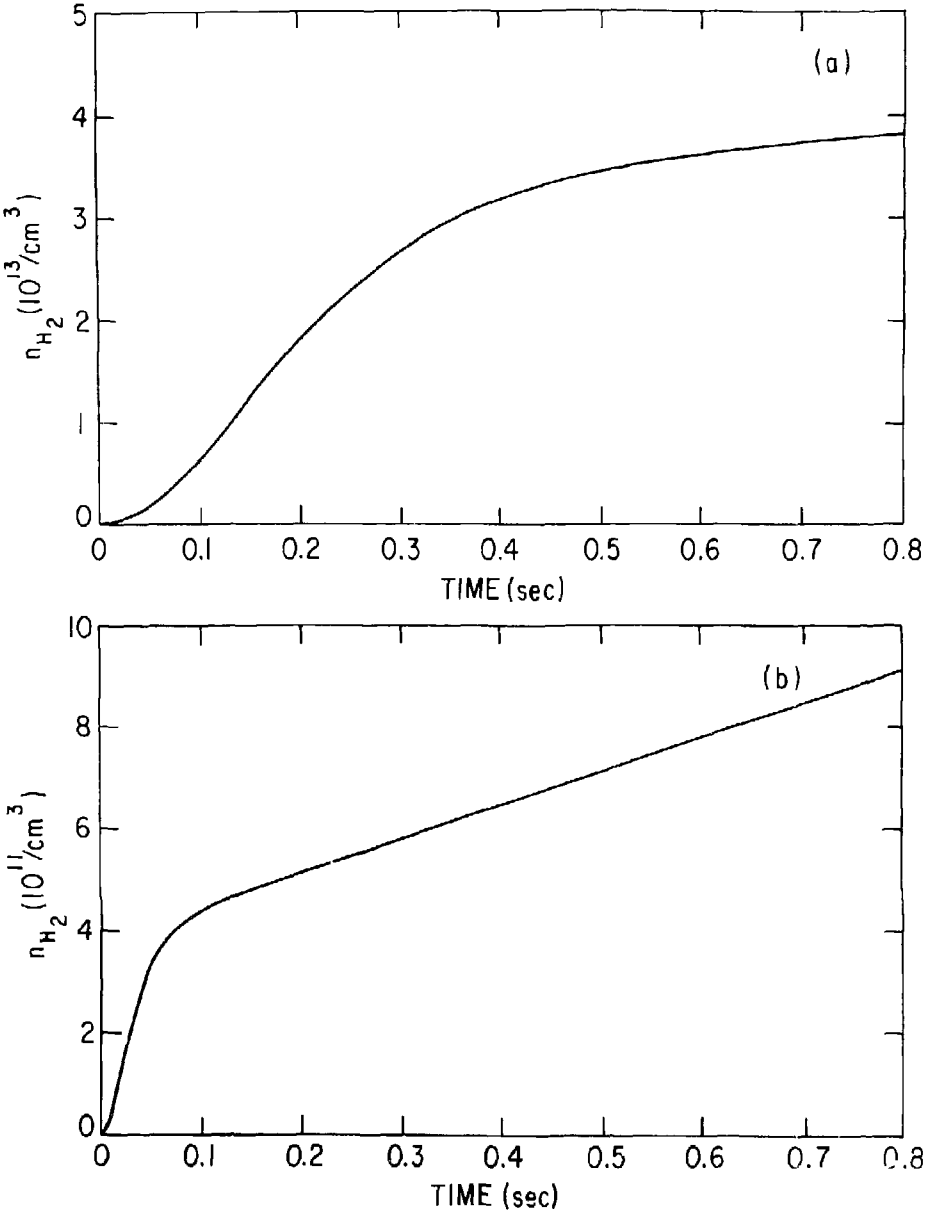

Fig. 12. (PPPL-803018)

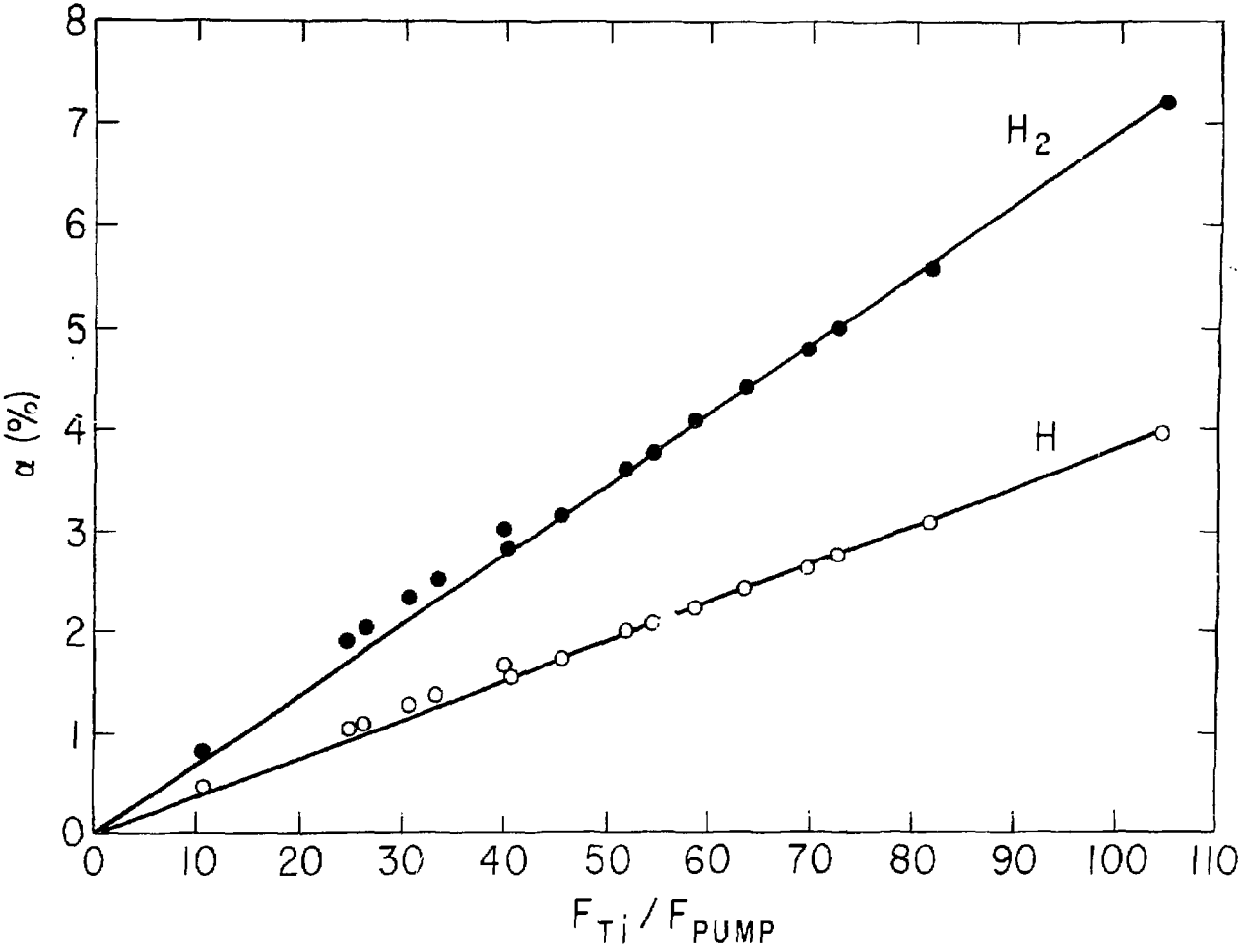

Fig. 13. (PPPL-793802)

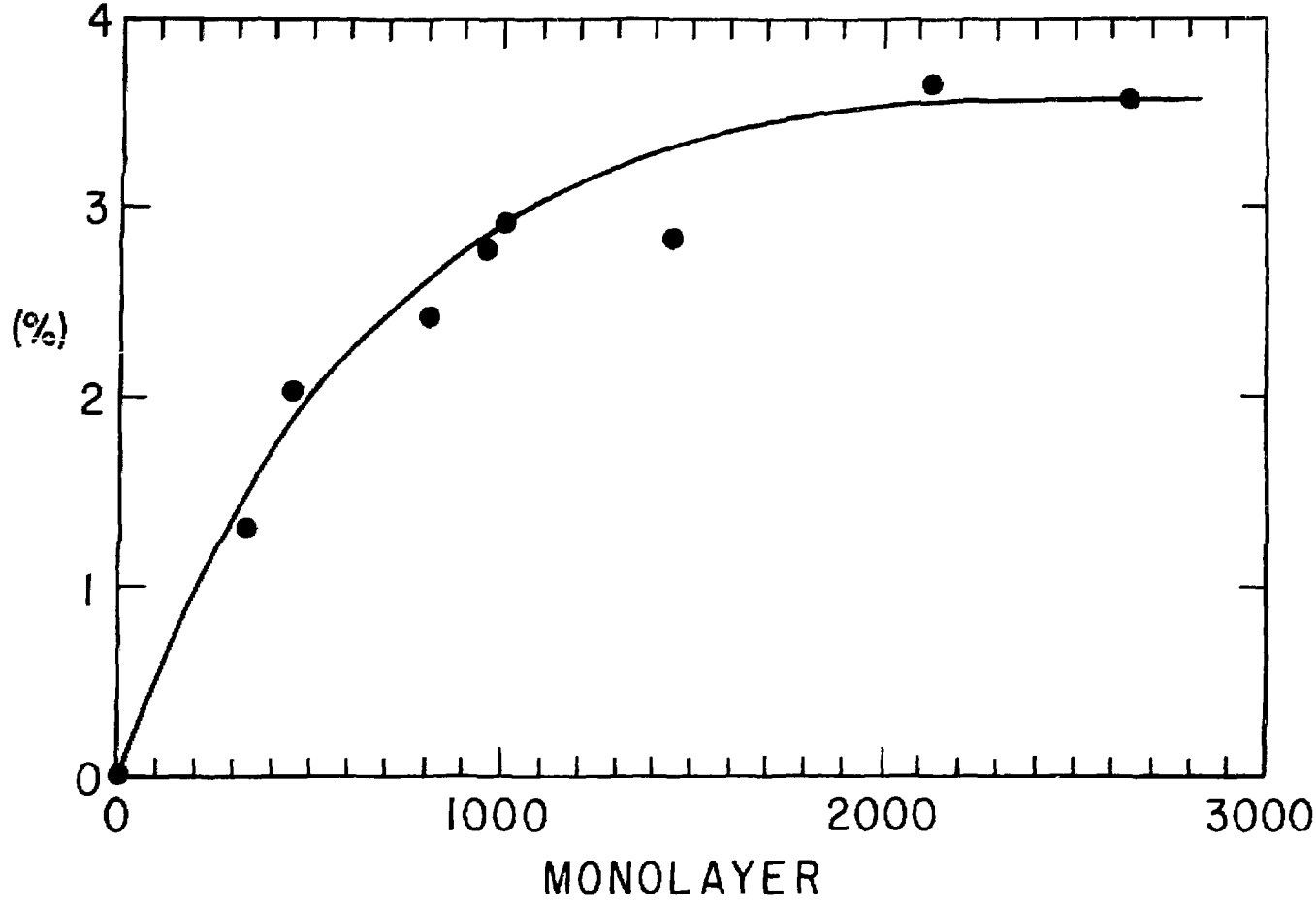

Fig. 14. (PPPL-793803)

EXTERNAL DISTRIBUTION IN ADDITION TO TID UC-20

ALL CATEGORIES

R. Askew, Auburn University, Alabama
S. T. Wu, Univ. of Alabama
Geophysical Institute, Univ. of Alaska
G.L. Johnston, Sonoma State Univ, California
H. H. Kuehl, Univ. of S. California
Institute for Energy Studies, Stanford University
H. D. Campbell, University of Florida
N. L. Oleson, University of South Florida
W. M. Stacey, Georgia Institute of Technology
Benjamin Ma, Iowa State University
Magne Kristiansen, Texas Tech. University
W. L. Wiese, Nat'l Bureau of Standards, Wash., D.C.
Australian National University, Canberra
C.N. Watson-Munro, Univ. of Sydney, Australia
F. Cap, Inst. for Theo. Physics, Austria
Dr.M. Heindler, Institute for Theoretical Physics Technical University of Graz
Ecole Royale Militaire, Bruxelles, Belgium
D. Palumbo, C. European Comm. B-1049-Brussels
P.H. S. Canaka, Instituto de Fisica, Campinas, Brazil
M.P. Bachynski, MPB Tech., Ste. Anne de Bellevue, Quebec, Canada
C. R. James, University of Alberta, Canada
T.W. Johnston, INRS-Energie, Varennes, Quebec
H. M. Skarsgard, Univ. of Saskatchewan, Canada
Inst. of Physics, Academia Sinica, Peking, People's Republic of China
Inst. of Plasma Physics, Hefei, Anhwei Province, People's Republic of China
Library, Tsing Hua Univ., Peking, People's Republic of China
Zhengwu Li, Southwestern Inst. of Phys., Leshan, Sichuan Province, People's Republic of China
Librarian, Culham Laboratory, Abingdon, England (2)
A.M. Dupas Library, C.E.N.-G, Grenoble, France
Central Res. Inst. for Physics, Hungary
S. R. Sharma, Univ. of Rajasthan, JAIPUR-4, India
R. Shingal, Meerut College, India
A.K. Sundaram, Phys. Res. Lab., India
Biblioteca, Frascati, Italy
Biblioteca, Milano, Italy
G. Rostagni, Univ. Di Padova, Padova, Italy
Preprint Library, Inst. de Fisica, Pisa, Italy
Library, Plasma Physics Lab., Gokasho, Uji, Japan
S. Mori, Japan Atomic Energy Res. Inst., Tokai-Mura
Research Information Center, Nagoya Univ., Japan
S. Shioda, Tokyo Inst. of Tech., Japan
Inst. of Space & Aero. Sci., Univ. of Tokyo
T. Uchida, Univ. of Tokyo, Japan
H. Yamato, Toshiba R. & D. Center, Japan
M. Yoshikawa, JAERI, Tokai Res. Est., Japan
Dr. Tsuneo Nakakita, Toshiba Corporation, Kawasaki-Ku Kawasaki, 210 Japan
N. Yajima, Kyushu Univ., Japan
R. England, Univ. Nacional Auto-noma de Mexico
B. S. Liley, Univ. of Waikato, New Zealand
S. A. Moss, Saab Univas Norge, Norway
J.A.C. Cabral, Univ. de Lisboa, Portugal
O. Petrus, AL.I. CUZA Univ., Romania
J. de Villiers, Atomic Energy Bd., South Africa
A. Maurech, Comisaria De La Energy y Recoursos Minerales, Spain
Library, Royal Institute of Technology, Sweden
Cen. de Res. En Phys.Des Plasmas, *Switzerland*
Librarian, Fom-Instituut Voor Plasma-Fysica, The Netherlands
Bibliothek, Stuttgart, West Germany
R.D. Bohler, Univ. of Stuttgart, West Germany
Max-Planck-Inst. fur Plasmaphysik, W. Germany
Nucl. Res. Estab., Julich, West Germany
K. Schindler, Inst. Fur Theo. Physik, W. Germany

EXPERIMENTAL THEORETICAL

M. H. Brennan, Flinders Univ. Australia
H. Barnard, Univ. of British Columbia, Canada
S. Sreenivasan, Univ. of Calgary, Canada
J. Radet, C.E.N.-B.P., Fontenay-aux-Roses, France
Prof. Schatzman, Observatoire de Nice, France
S. C. Sharma, Univ. of Cape Coast, Ghana
R. N. Aiyer, Laser Section, India
B. Buti, Physical Res. Lab., India
L. K. Chavda, S. Gujarat Univ., India
I.M. Das Das, Banaras Hindu Univ., India
S. Cuperman, Tel Aviv Univ., Israel
E. Greenspan, Nuc. Res. Center, Israel
P. Rosenau, Israel Inst. of Tech., Israel
Int'l. Center for Theo. Physics, Trieste, Italy
I. Kawakami, Nihon University, Japan
T. Nakayama, Ritsumeikan Univ., Japan
S. Nagao, Tohoku Univ., Japan
J.I. Sakai, Toyama Univ., Japan
S. Tjotta, Univ. I Bergen, Norway
M.A. Hellberg, Univ. of Natal, South Africa
H. Wilhelmsson, Chalmers Univ. of Tech., Sweden
Astro. Inst., Sonnenborgh Obs., The Netherlands
T. J. Boyd, Univ. College of North Wales
K. Hubner, Univ. Heidelberg, W.Germany
H. J. Kaeppeler, Univ. of Stuttgart, West Germany
K. H. Spatschek, Univ. Essen, West Germany

EXPERIMENTAL ENGINEERING

B. Grek, Univ. du Quebec, Canada
P. Lukac, Komenskeho Univ., Czechoslovakia
G. Horikoshi, Nat'l Lab for High Energy Physics, Tsukuba-Gun, Japan

EXPERIMENTAL

F. J. Paoloni, Univ. of Wollongong, Australia
J. Kistemaker, Fom Inst. for Atomic & Molec. Physics, The Netherlands

THEORETICAL

F. Verheest, Inst. Vor Theo. Mech., Belgium
J. Teichmann, Univ. of Montreal, Canada
T. Kalvan, Univ. Paris VII, France
R. K. Chhajlani, India
S. K. Trehan, Panjab Univ., India
T. Namikawa, Osaka City Univ., Japan
H. Narumi, Univ. of Hiroshima, Japan
Korea Atomic Energy Res. Inst., Korea
E. T. Karlson, Uppsala Univ., Sweden
L. Stenflo, Univ. of UMEA, Sweden
J. R. Saraf, New Univ., United Kingdom